Available online at www.sciencedirect.com
SCIENCE DIRECT®
Acta Materialia 53 (2005) 1085–1096
Acta MATERIALIA
www.actamat-journals.com

Edge-to-edge matching and its applications Part II. Application to Mg–Al, Mg–Y and Mg–Mn alloys

M.-X. Zhang *, P.M. Kelly

Division of Materials, School of Engineering, The University of Queensland, St. Lucia, Qld. 4072, Australia

Received 22 July 2004; received in revised form 29 October 2004; accepted 2 November 2004
Available online 8 December 2004

Abstract

A model for the crystallography and morphology of diffusion-controlled phase transformations – edge-to-edge matching – has been used to predict the orientation relationships (OR) and habit planes of precipitates $Mg_{17}Al_{12}$ in Mg–Al alloy, $Mg_{24}Y_5$ in Mg–Y alloy and α-Mn in Mg–Mn alloy. Based on the crystal structures and lattice parameters only, the model predicts that the possible ORs between $Mg_{17}Al_{12}$ and Mg matrix are the near Burgers OR, the Potter OR, the Gjönnes–Östmoe OR and the Crawley OR. In the Mg–Y alloy, the OR between $Mg_{24}Y_5$ precipitates and the Mg matrix is predicted to be the Burgers OR only. The model also predicts that there are no reproducible ORs between α-Mn and Mg in the Mg–Mn alloy. Combining the edge-to-edge matching model and W. Zhang's **Δg** approach, the habit plane and side facets of the precipitate for each OR can be determined. All the predicted ORs and the corresponding habit planes in Mg–Al and Mg–Y alloys agree very well with the experimental results.

Keywords: Electron diffraction; Magnesium alloys; Interface structure; Phase transformation; Crystallography; Edge-to-edge matching

1. Introduction

As the lightest metallic structural alloy with a good combination of castability, mechanical properties and ductility, magnesium alloys have attracted increased attention over the last 10 years [1–5]. The lightness of the metal has led to more and more applications in the automotive and aerospace industries [5–7]. Among the commercial magnesium alloys, AZ91 (Mg–9wt%Al–0.5/1.0wt%Zn–0.3wt%Mn) is the most popular and extensive research has been carried out on this alloy [8–13]. In AZ91, the intermetallic compound $Mg_{17}Al_{12}$ (β phase) is the only precipitate generated during ageing after solution treatment. Previous research [1,8,10,12,13] has shown that both the continuous and the discontinuous β precipitates in AZ91 alloy have the same crystallographic features. The reported predominant orientation relationship (OR) between the β phase, which has a body-centered cubic (BCC) crystal structure, and the hexagonal close packed (HCP) magnesium matrix is the Burgers OR [1,8,10,12].
The Burgers OR:

$$(0001)_H \| (011)_B \quad \text{and} \quad [2\bar{1}\bar{1}0]_H \| [1\bar{1}1]_B,$$

where B denotes BCC and H denotes HCP.

The habit plane corresponding to this OR is $(0001)_H$, the basal plane of the matrix. In addition, Duly et al. [1] reported that in the OR between the β phase and Mg matrix the $(0001)_H$ plane is strictly parallel to the $(011)_B$ plane, but the directions $[2\bar{1}\bar{1}0]_H$ and $[1\bar{1}1]_B$ are either strictly parallel or deviate from each other by 0.5°. This deviation leads to the angle between $[11\bar{2}0]_H$ and $[100]_B$ increasing from 5.26° in the exact Burgers OR to 5.76°. For convenience, this OR is termed the near Burgers OR in the present paper and can be expressed as:

* Corresponding author. Tel.: +61 733 65 3669; fax: +61 733 65 3888.
E-mail address: m.zhang@minmet.uq.edu.au (M.-X. Zhang).

1359-6454/$30.00
doi:10.1016/j.actamat.2004.11.005

The near Burgers OR:

$(0001)_H \| (011)_B$, $[2\bar{1}\bar{1}0]_H 0.5^\circ$ from $[1\bar{1}1]_B$.

Recently, Zhang and Kelly [13] used the more accurate Kikuchi line diffraction technique to determine the OR between the β phase and the magnesium matrix and the corresponding habit planes in AZ91. Careful examination of the results in Fig. 2 of [13] shows that in more than 40 experimental results, the deviation of $[2\bar{1}\bar{1}0]_H$ from $[111]_B$ is real. The average deviation is 0.52°. Hence we believe that the exact Burgers OR and the near Burgers OR are two of the predominant ORs between the Mg matrix and the β phase in Mg–Al alloy. Zhang and Kelly [13] also reported the Potter OR that was equally observed. The Potter OR is as follows:
The Potter OR:

$(0001)_H 2^\circ$ from $(011)_B$, $(01\bar{1}1)_H \| (110)_B$, $[2\bar{1}\bar{1}0]_H \| [1\bar{1}1]_B$.

They also determined the lattice parameters of individual precipitates using Kikuchi line diffraction patterns [13–15] and found that the lattice parameter of precipitates associated with the Potter OR ranged from 1.050 to 1.058 nm, while it was between 1.063 and 1.069 nm for the precipitates that obeyed the Burgers OR. The habit plane associated with the Burgers OR is $(0001)_H \| (011)_B$, and the habit planes for the Potter OR are more complicated. Approximately, the determined results are close to one of the following three habit planes within a range of 16°: $(10\bar{1}1)_H \| (101)_B$, $(\bar{1}\bar{2}30)_H \| (11\bar{1})_B$ and $(0001)_H \| (01\bar{1})_B$ [13]. These results indicate that the lattice parameters of the precipitates not only affect the OR, but also affect the habit planes.

Zhang and Kelly [16] also determined the OR between $Mg_{24}Y_5$ (ε phase) and the Mg matrix and the corresponding habit planes in a Mg–10.2wt%Y alloy. The ε phase has the same crystal structure as β phase, but with a 6.8% increase in lattice parameter (a = 1.126). The Burgers OR with habit plane between $\{10\bar{1}0\}_H$ and $\{31\bar{4}0\}_H$ was observed for all precipitates in this alloy. This result further proves the significant effect of lattice parameters on the crystallographic features of precipitation in magnesium alloys. The question that arises here is how the lattice parameter governs the OR and the habit plane in these two alloys. The aim of the present paper is to use the recently developed edge-to-edge matching model [17] to rationalize the observed crystallographic features of the β and the ε phases in magnesium alloys. In order to further understand this system, the crystallographic features of α-Mn precipitates and Mg matrix in Mg–Mn alloys were also studied.

In addition, other ORs were also observed in Mg–Al based alloys. For the precipitates that are rod-shaped with their long direction either perpendicular to or inclined to basal plane, three ORs have been reported [10,12,18,19]:

The Gjönnes–Östmoe (G–O) OR:

$(0001)_H \| (011)_B$, $[11\bar{2}0]_H \| [21\bar{1}]_B$.

The Porter OR:

$(\bar{1}\bar{1}21)_H \| (011)_B$, $[1\bar{1}00]_H \| [0\bar{1}1]_B$.

The Crawley OR:

$(0001)_H \| (1\bar{1}1)_B$, $(10\bar{1}0)_H \| (110)_B$, $[1\bar{2}10]_H \| [\bar{1}12]_B$.

Precipitates obeying these ORs lie on the prism plane of the Mg matrix with a habit plane of $\{1\bar{1}00\}_H$.

2. Experimental

The experimental process for Mg–Al and Mg–Y alloys has been described in [13] and [16]. The chemical composition of the Mg–Mn alloy was Mg–1.4wt%Mn. The alloy was made by melting pure Mg metal in a steel crucible at 780 °C with additions of very fine Mn metal chips, followed by holding for 4 h, and then casting into a 25 mm diameter ingot in a steel mould. Block specimens were cut from the ingot, solution treated at 620 °C for 12 h under the protection of SF_6 flux followed by water quench, and then aged at 400 °C for 6 h.

Slices 0.8–1.0 mm thick were cut from the block specimens using a diamond-cutting blade. After mechanical grinding to 0.08–0.1 mm thick, 3 mm diameter disks were punched from the foil. The disks were then jet polished in a solution of 10.6 g lithium chloride, 22.32 g magnesium perchlorate, 1000 ml methanol and 100 ml 2-butoxy-ethanol at −55 °C with a voltage of 75 V. Jet polishing was stopped just before perforation. Then TEM specimens were thinned by ion milling until a hole appeared. All thin foils were immediately examined in a Tecnai 20 FEG TEM.

ORs were determined using Kikuchi line diffraction patterns [20–21]. The habit plane of each precipitate was determined using the trace width method [14].

3. Experimental results

ORs and the corresponding habit planes in both the Mg–Al alloys and the Mg–Y alloy have been reported previously [1,8–13,16] and have been summarized above. In the present work, crystallographic results obtained in a Mg–Mn alloy are presented. A total of 21 different Mn precipitates in the Mg–Mn alloy were examined after the heat treatment described above and it was found that no reproducible ORs were observed for these 21 precipitates. Fig. 1 shows a typical TEM microstructure of a Mn precipitate and the corresponding Kikuchi line dif-

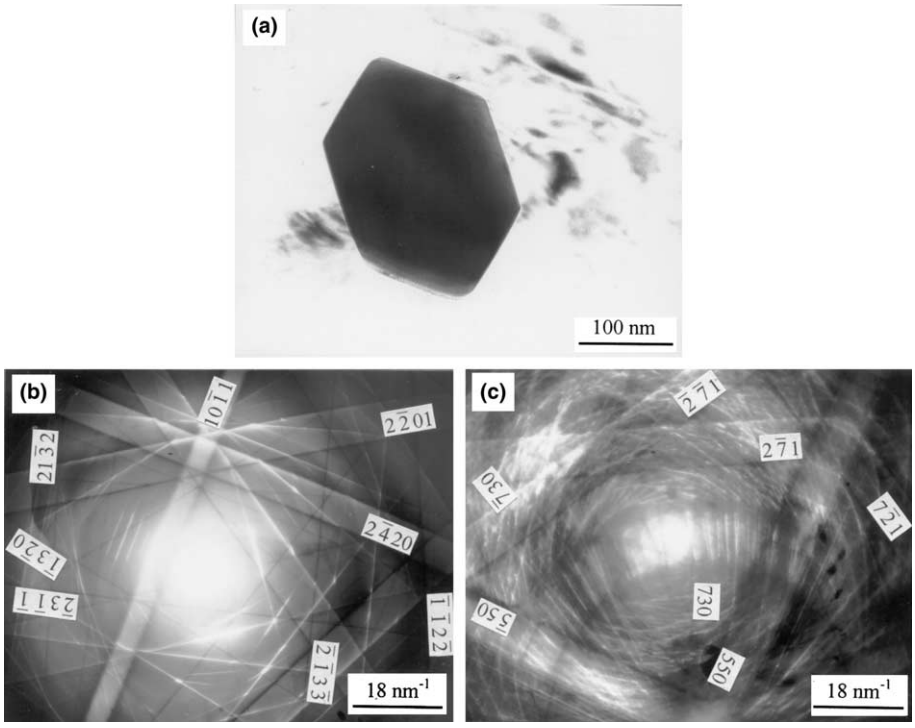

Fig. 1. Typical regular shaped α-Mn precipitate in Mg–1.4wt%Mn alloy after 620 °C solution treatment for 12 h followed by 400 °C ageing for 6 h: (a) TEM micrograph; (b) Kikuchi pattern from Mg matrix; and (c) Kikuchi pattern from α-Mn precipitate.

fraction patterns. The OR showing in Fig. 1 (b) and (c) is: $(0001)_H$ 6.8° from $(\bar{5}11)_B$, $[1\bar{1}00]_H$ 4.3° from $[0\bar{1}1]_B$, which is not a typical, simple OR. All the ORs determined in the 21 precipitates were different from each other. Hence, it is considered that even though the Mn precipitates have regular shape, no meaningful OR exists between α-Mn and the Mg matrix.

4. Predictions of the edge-to-edge matching model

To predict the ORs and the corresponding habit planes, the crystal structure, lattice parameters and the atom positions of the precipitates and matrix are the only data required. In all three alloys, the Mg matrix has a hexagonal structure. According to Vegard's law [22–24], the lattice parameters of Mg vary linearly with its chemical composition. However, because the amount of solute element in solid solution in Mg is very low after the precipitation of the intermetallic compounds (β, ε, α-Mn), the effect of the solute element on the lattice parameters of Mg matrix can be ignored. The lattice parameters of pure Mg metal are used in the present work. These are $a = 0.320936$ nm and $c = 0.521123$ nm [25]. As the chemical composition of the β phase varies over quite a large range according to the Mg–Al phase diagram [26], the effect of chemical composition on the lattice parameter of $Mg_{17}Al_{12}$ has to be taken into account. The data used were determined in previous work [13], and showed a variation between 1.050 and 1.069 nm. Due to the small variation in chemical composition of the ε phase and α-Mn, the lattice parameters [25], $a = 1.126$ nm for ε phase and $a = 0.89125$ nm for α-Mn were used.

4.1. Possible matching directions and matching planes in HCP and BCC phases

According to the edge-to-edge matching model [17,27], the matching directions and matching planes are normally the close packed or nearly close packed directions and planes. As a simple HCP structure, Mg has three possible close or nearly close packed directions. These are $\langle 11\bar{2}0\rangle_H$, $\langle 10\bar{1}0\rangle_H$ and $\langle 11\bar{2}3\rangle_H$. The first direction is a straight atom row and the other two are zigzag atom rows [27]. The possible close or nearly close packed directions in BCC structure precipitates are associated with atom positions in the unit cell due to the complex crystal structure. This will be described in the following sections. Normally they should be the directions with low indices, such as $\langle 111\rangle_B$, $\langle 110\rangle_B$, $\langle 100\rangle_B$, $\langle 112\rangle_B$ and $\langle 113\rangle_B$. The close packed or nearly close packed planes of Mg can be identified either through the calculation of the structure factors, or by empirical examination of the powder X-ray diffraction intensity available from the PDF file [25]. The biggest structure factor or the highest intensity of the X-ray diffraction corresponds to the closest packed plane. For

pure Mg, the three close or nearly close packed planes are $\{10\bar{1}1\}_H$, $\{0002\}_H$ and $\{10\bar{1}0\}_H$. For the complex BCC precipitates (β phase, ε phase and α-Mn), with the same structure type, there are two close or nearly close packed planes, $\{330\}_B$ and $\{332\}_B$. Hence, there are six combinations of matrix/precipitate plane pairs, $\{10\bar{1}1\}_H/\{330\}_B$, $\{0002\}_H/\{330\}_B$, $\{10\bar{1}0\}_H/\{330\}_B$, $\{10\bar{1}1\}_H/\{332\}_B$, $\{0002\}_H/\{332\}_B$ and $\{10\bar{1}0\}_H/\{332\}_B$.

4.2. Mg–Al alloy

One unit cell of β phase precipitated contains 34 Mg atoms and 24 Al atoms. The atom positions [28] are listed in Table 1.

Based on these atom positions, Fig. 2 shows the atom configurations on the $(\bar{1}10)_B$ plane with the lattice parameter $a = 1.05438$ nm [28]. Because this plane contains all possible close packed or nearly close packed directions, the matching directions may be identified from this figure. The notation Al_R refers to Al atoms, which do not exactly lie in the plane, but where the distance from the atom center to the plane is less than the atomic radius. All other atoms (Al and Mg) have atom centers that are exactly in the plane. From Fig. 2 it can be seen that along directions, $[001]_B$ and $[112]_B$, the interatomic spacing is rather large or particularly variable. Therefore, these two directions are unlikely to be good matching directions and will be excluded from further consideration. The close packed or nearly close packed directions that can be potential matching directions are $\langle 111\rangle_B$, $\langle 110\rangle_B$ and $\langle 113\rangle_B$. But the atomic configurations along these directions are quite different. The first two directions can be considered as straight atom rows since all the atoms do not deviate significantly from the overall direction. The third case $\langle 113\rangle_B$ is more complicated. Along this direction there are straight portions and zigzag portions, which implies that this direction has both the features of a straight row and a zigzag row. Following the rules adopted with the simple BCC structure [29], namely that straight rows match with straight rows and zigzag rows with zigzag rows, the straight row matching condition leads to two matching direction pairs. These are $\langle 11\bar{2}0\rangle_H/\langle 111\rangle_B$ and $\langle 11\bar{2}0\rangle_H/\langle 110\rangle_B$. Because of its versatile nature,

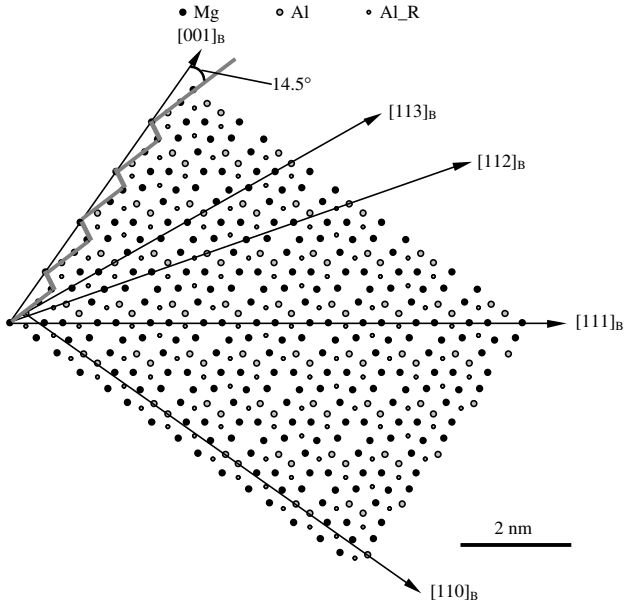

Fig. 2. Atom configuration of the β phase in the $(\bar{1}10)_B$ plane at $a = 1.05438$ nm.

the $\langle 113\rangle_B$ direction can match with either a straight row or a zigzag row. This results in three possible matching direction pairs: $\langle 11\bar{2}0\rangle_H/\langle 113\rangle_B$, $\langle 10\bar{1}0\rangle_H/\langle 113\rangle_B$ and $\langle 11\bar{2}3\rangle_H/\langle 113\rangle_B$. The interatomic spacing along a particular direction is related to the lattice parameter, so the interatomic spacing misfit along each direction pair will also vary with the lattice parameters. The variation of interatomic misfit along these five possible matching direction pairs with the lattice parameter of the β phase is shown in Fig. 3. If, as stated in Part I [29], 10% is selected as the critical value of the interatomic spacing misfit, it can be seen from Fig. 3 that all these five matching direction pairs satisfy this condition. However, when the lattice parameter of the β phase is less than 1.058 nm, the most preferred OR will be generated from the matching direction pair $\langle 10\bar{1}0\rangle_H/\langle 113\rangle_B$, and when the lattice parameter is over 1.058 nm, the most preferred OR will be associated with the matching direction pair $\langle 11\bar{2}3\rangle_H/\langle 113\rangle_B$. All other matching directions are also possible and may form an OR, probably with less frequency of appearance than the most preferred OR. The lowest priority to form an

Table 1
Atom position in $Mg_{17}Al_{12}$β phase

Structure type: Mn	Pearson symbol: *cI*58	Space group: $I\bar{4}m$	Space group no. 217
Multiplicity, Wyckoff letter, Site symmetry	Coordinates: (0,0,0,)+ (0.5,0.5,0.5)+		
	x	*y*	*z*
Mg1, 2*a*, $\bar{4}3m$	0	0	0
Mg2, 8*c*, *.m*	0.3240	0.3240	0.3240
Mg3, 24*g*, *..m*	0.3582	0.3582	0.0393
Al, 24*g*, *..m*	0.0954	0.0954	0.2725

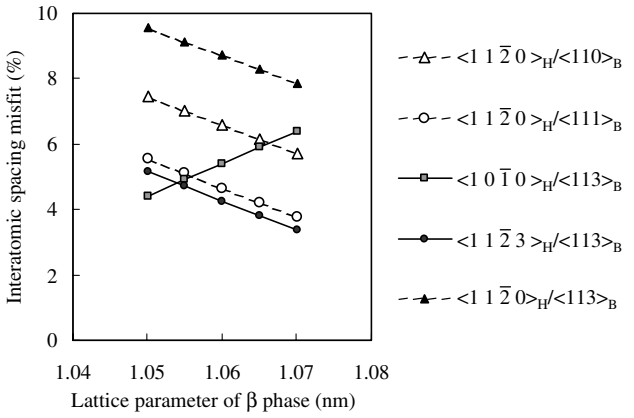

Fig. 3. Variation of interatomic spacing misfit in different matching directions with the lattice parameter of the β phase in Mg–Al alloy.

OR are the matching direction pairs, $\langle 11\bar{2}0\rangle_H/\langle 113\rangle_B$ and $\langle 11\bar{2}0\rangle_H/\langle 110\rangle_B$.

Once the matching directions are defined, the *d*-value mismatch between the possible matching planes that contain these matching directions needs to be examined. Like the interatomic spacing, the *d*-value mismatch between plane pairs varies with the lattice parameter of β phase. Fig. 4 shows this variation for the six plane pairs selected above. If 6% is used as the critical data of the *d*-value mismatch to form an OR [29], the plane pairs involving the $\{332\}_B$ plane are outside this range. Normally, the plane pair that results in a *d*-value mismatch greater than 6%, will not be considered as a matching plane unless it is the smallest *d*-value mismatch of all plane pairs for a given matching direction. Thus, only the plane pairs, $\{10\bar{1}1\}_H/\{330\}_B$ and $\{0002\}_H/\{330\}_B$, have the potential to be the matching planes to form an OR. The actual ORs and the corresponding habit planes now can be predicted.

The matching direction pair, $\langle 11\bar{2}0\rangle_H/\langle 111\rangle_B$, is related to two ORs, $\langle 11\bar{2}0\rangle_H\|\langle 111\rangle_B$, $\{0002\}_H\|\{\bar{3}30\}_B$ and $\langle 11\bar{2}0\rangle_H\|\langle 111\rangle_B$, $\{1\bar{1}01\}_H\|\{\bar{3}30\}_B$, which are actually the ideal Burgers OR and the ideal Potter OR. Using the **Δg** theory [1,30–35] and the computer program developed to further refine these ORs, as described before [27,29], the actual ORs that are predicted between the β phase and the Mg matrix in real materials and the corresponding habit planes can be obtained. They are:

$$[11\bar{2}0]_H\|[111]_B \quad (0002)_H \ -2.23^\circ \text{ from } (\bar{3}30)_B \quad [\bar{1}2\bar{1}0]_H \ 5.58^\circ \text{ from } [001]_B, \tag{1}$$

$$[11\bar{2}0]_H\|[111]_B \quad (1\bar{1}01)_H \ 0.3^\circ \text{ from } (\bar{3}30)_B \quad [2\bar{1}\bar{1}0]_H \ 5.58^\circ \text{ from } [010]_B. \tag{2}$$

OR (1) corresponds a habit plane that is 2.6° from $(\bar{3}12)_B \sim \|(\bar{1}102)_H$. OR (2) has the habit plane that is 2.6° from $(\bar{3}21)_B \sim \|(1\bar{1}02)_H$. It can be seen that both OR (1) and OR (2) are actually the Potter OR [13,19], in which the $[2\bar{1}\bar{1}0]_H$ is 5.51° away from $[010]_B$ and both correspond to the same habit plane as well. Although the habit plane is not consistent with the results previously published by the present authors [13], it has been reported by Duly et al. [1]. Fig. 5 shows the simulated diffraction patterns along the zone axis $[11\bar{2}0]_H\|[111]_B$ for the OR (1) with at least two parallel **Δg**s. The dashed line indicates the habit plane. It should be mentioned that the diffraction patterns include all forbidden reflections for this purpose [29]. A similar superimposed diffraction patterns for the OR (2) can also be constructed, but in the interests of brevity will not be shown here.

The matching direction, $\langle 10\bar{1}0\rangle_H/\langle 113\rangle_B$, leads to one OR only, namely $\langle 10\bar{1}0\rangle_H\|\langle 113\rangle_B$ and $\{0002\}_H\|\{\bar{3}30\}_B$. Because this can be regarded as a Type I zigzag row matching with a Type I zigzag row, the rotation angle of the matching plane resulting from the refinement

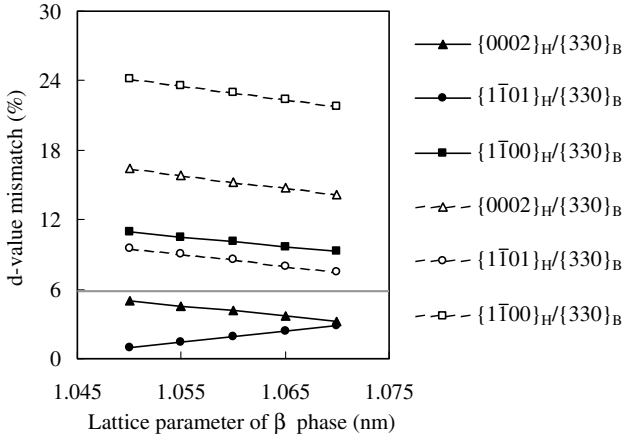

Fig. 4. Variation of *d*-value mismatch between possible matching planes with the lattice parameter of β phase in Mg–Al alloy.

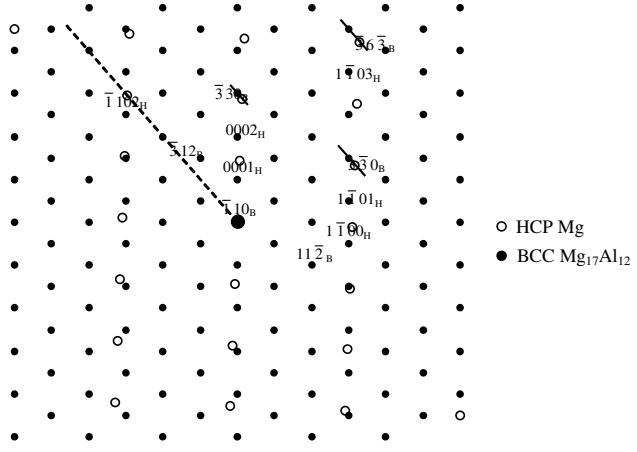

Fig. 5. Simulated diffraction patterns of Mg matrix and β phase along the zone axis $[11\bar{2}0]_H\|[111]_B$, showing the OR (1), and a set of parallel **Δg**s.

would have to be small. After the refinement using the **Δg** approach with a 0.63° rotation of the matching plane about the matching direction, the following OR is obtained:

$$[2\bar{1}\bar{1}0]_H\ 0.59^\circ \text{ from } [111]_B \quad (0002)_H\ 0.63^\circ \text{ from } (\bar{3}30)_B$$
$$[11\bar{2}0]_H\ 4.77^\circ \text{ from } [001]_B \qquad (3)$$

with a habit plane that is 12.8° from $(3\bar{3}0)_B \sim \|(0002)_H$. Compared with the ideal Burgers OR that is $[2\bar{1}\bar{1}0]_H\|[111]_B$, $(0002)_H\|(3\bar{3}0)_B$, $[11\bar{2}0]_H$ 5.26° from $[001]_B$, OR (3) is actually one version of the near Burgers OR, which rotated from the ideal Burgers OR by 0.59° towards $[11\bar{2}0]_H$. The predicted habit plane is also very close to the experimentally determined habit plane for the reported Burgers OR. Fig. 6 is the simulated diffraction patterns (including the forbidden reflections) showing this OR and a set of parallel **Δg**s.

The matching direction, $\langle 11\bar{2}3\rangle_H/\langle 113\rangle_B$, also results in only one OR, $\langle 11\bar{2}3\rangle_H\|\langle 113\rangle_B$, $\{0\bar{1}11\}_H\|\{\bar{3}30\}_B$. Because this direction matching is between a Type I zigzag row and a Type II zigzag row, a larger rotation angle of the matching plane after the refinement can be allowed. This leads to an OR with −9.98° rotation about the matching direction through the use of **Δg** approach. This OR is

$$[2\bar{1}\bar{1}0]_H\ 0.51^\circ \text{ from } [111]_B \quad (0002)_H\ 0.34^\circ \text{ from } (\bar{3}30)_B$$
$$[11\bar{2}0]_H\ 5.77^\circ \text{ from } [001]_B \qquad (4)$$

with a habit plane close to $(\bar{1}4\bar{3}\bar{1})_H \sim \|(\bar{2}\bar{3}3)_B$, which is about 10° from $(1\bar{3}20)_H\|(\bar{1}\bar{1}1)_B$. Compared with the ideal Burgers OR, this is another version of the near Burgers OR. The difference between OR (3) and OR (4) is that the latter deviates from the ideal Burgers OR by 0.51° towards the $[1\bar{2}10]_H$ direction and the former towards the $[11\bar{2}0]_H$ direction. The latter leads to the angle between $[11\bar{2}0]_H$ and $[001]_B$ increasing and the former makes it smaller. The predicted habit plane for OR (4) is different from the normally reported habit plane for the Burgers OR [8–12], which is the basal plane of the HCP matrix. But the present authors [13] have reported a habit plane for the near Burgers OR that is very close to the predicted one, even though it has not been observed frequently. Another important observation is that, as shown in Fig. 3, OR (4) is the most likely relationship to form when the lattice parameter of β phase is larger then 1.058 nm. When the **Δg** theory was applied to this matching direction, no OR was generated until the lattice parameter of β phase exceeded 1.06 nm. Fig. 7 is the simulated diffraction pattern along the zone axis $[\bar{2}113]_H\|[\bar{3}1\bar{1}]_B$ (including the forbidden reflections) showing this OR and a set of parallel **Δg**s.

The matching direction, $\langle 11\bar{2}0\rangle_H/\langle 113\rangle_B$, has two plane pairs, and therefore leads to two cases. They are $\langle 11\bar{2}0\rangle_H\|\langle 113\rangle_B$ $\{1\bar{1}01\}_H\|\{330\}_B$ and $\langle 11\bar{2}0\rangle_H\|\langle 113\rangle_B$, $\{0002\}_H\|\{330\}_B$. Applying the **Δg** theory to case 1, the following OR obtained is

$$[11\bar{2}0]_H\|[113]_B, \quad (1\bar{1}01)_H 0.05^\circ \text{ from } (\bar{3}30)_B. \qquad (5)$$

This is an unusual OR and has never been observed in the HCP/BCC system. For case 2, the refined OR is

$$[\bar{2}110]_H\ 0.79^\circ \text{ from } [11\bar{2}]_B \quad (0002)_H\ 0.7^\circ \text{ from } (\bar{3}30)_B. \qquad (6)$$

It corresponds to a habit plane that is close to $(2\bar{1}0)_B \sim \|(\bar{1}105)_H$. OR (6) is actually the Gjönnes–Östmoe OR that was observed when the β phase is an angle to the basal plane of the Mg matrix [12]. The predicted habit plane is also consistent with the experimental results. Similar superimposed diffraction patterns can

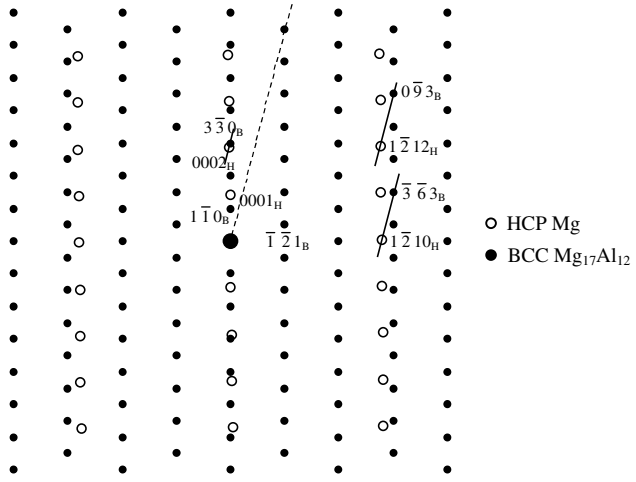

Fig. 6. Simulated diffraction patterns of Mg matrix and β phase along the zone axis $[10\bar{1}0]_H\|[113]_B$, showing the OR (3) and a set of parallel **Δg**s. Dashed line indicates the habit plane.

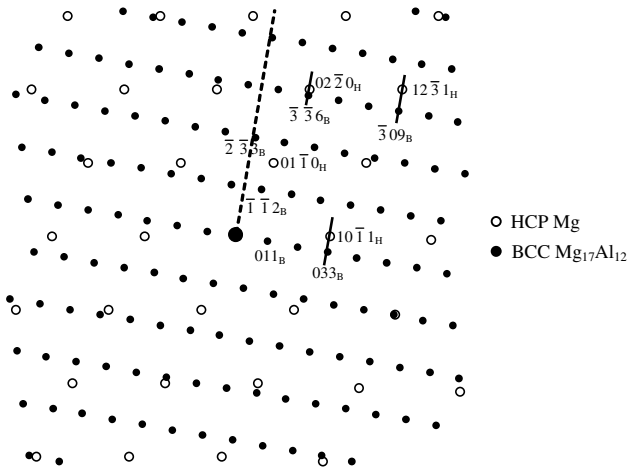

Fig. 7. Simulated diffraction patterns of Mg matrix and β phase along the zone axis $[\bar{2}113]_H\|[\bar{3}1\bar{1}]_B$, showing the OR (4) and a set of parallel **Δg**s. Dashed line indicates the habit plane.

be used to show this OR and the parallel **Δg**s. In the interests of brevity this is not included in the paper.

The last matching direction $\langle 11\bar{2}0\rangle_H/\langle 110\rangle_B$ also involves two cases with the matching planes $\{1\bar{1}01\}_H \| 330_B$ and $\{0002\}_H \| \{330\}_B$. Further refinement gives following ORs:

$$[2\bar{1}\bar{1}0]_H \ 6.8^\circ \text{ from } [11\bar{2}]_B \quad (0002)_H \ 5.1^\circ \text{ from } (3\bar{3}0)_B. \tag{7}$$

Although it is close to the G–O OR, like OR (5), OR (7) it is not a recognized OR. The second case of this matching direction gives another OR that has not been observed:

$$[11\bar{2}0]_H \| [110]_B \quad (1\bar{1}01)_H \ -5.9^\circ \text{ from } (3\bar{3}0)_B. \tag{8}$$

From above analysis, eight ORs have been predicted using the model from first principles, using only the lattice parameters of both matrix and precipitate and the atom positions in the β phase. ORs (1) and (2) are actually the Potter OR that has been experimentally observed using accurate Kikuchi line diffraction techniques [13]. ORs (3) and (4) are two versions of the near Burgers OR, while OR (6) is the G–O OR. The other three ORs predicted from the matching directions $\langle 11\bar{2}0\rangle_H/\langle 113\rangle_B$ and $\langle 11\bar{2}0\rangle_H/\langle 110\rangle_B$ have never been found experimentally. In addition, from Fig. 3, it can be seen that, these two matching directions have the highest interatomic spacing misfit under the range of lattice parameters and atom positions used. Hence, the ORs (5), (7) and (8) formed from these matching directions are the least likely. In fact, as the atom row matching along $\langle 11\bar{2}0\rangle_H$ and $\langle 111\rangle_B$ leads to much lower interatomic spacing misfit, the chance for $\langle 11\bar{2}0\rangle_H$ to match $\langle 113\rangle_B$ or $\langle 110\rangle_B$ is extremely small. Thus, these ORs may never be observed unless the lattice parameters or the atom positions change. The ideal Burgers OR has been shown not to exist between the Mg matrix and the β phase. Instead, the reported ideal Burgers ORs are really the result of experimental errors in measuring what is really a near Burgers OR. Because the matching directions, $\langle 11\bar{2}3\rangle_H/\langle 113\rangle_B$ and $\langle 10\bar{1}0\rangle_H/\langle 113\rangle_B$, which form these two near Burgers ORs, are the most preferred matching directions, the two near Burgers ORs should be the predominate ORs in this system.

4.3. Mg–Y alloy

$Mg_{24}Y_5$ (ε phase) that precipitated from the Mg–Y alloy contains 48 Mg atoms and 10 Y atoms in one unit cell with the lattice parameter $a = 1.126$ nm [25]. The atom positions are listed in Table 2 [28]. Using these atom positions, the atom configurations on $(\bar{1}10)_B$, which contains all possible close or near close packed directions, can be constructed, as shown in Fig. 8. The notation Mg_R means the Mg atoms that are not exactly on the plane, but with the distance from the atom center to the plane being less than the atom radius. From Fig. 8 it can be seen that along the directions, $[001]_B$, $[112]_B$ and $[113]_B$, the interatomic spacing is large and variable. These directions are not close packed or nearly close packed directions in the ε phase and cannot be the matching directions. The close packed direction is $[111]_B$ and the nearly close packed direction is $[110]_B$. Both can be regarded as straight atom rows. Therefore, there will be two direction pairs that could be the possible matching directions. They are: $\langle 11\bar{2}0\rangle_H/\langle 110\rangle_B$ and $\langle 11\bar{2}0\rangle_H/\langle 111\rangle_B$. Table 3 lists the interatomic misfit along these two possible matching directions. If 10% is used as the critical value of the interatomic spacing misfit, obviously, the only possible matching directions is the direction pair, $[11\bar{2}0]_H \| [111]_B$. It involves three possible matching planes, $\{0002\}_H/\{\bar{3}30\}_B$, $\{1\bar{1}01\}_H/\{\bar{3}30\}_B$ and $\{1\bar{1}00\}_H/\{\bar{3}30\}_B$. The *d*-value mismatch between the planes of each pair is listed in Table 4.

If 6% is used as a critical value of *d*-value mismatch between matching planes to form an OR, there are two possible ORs. They are $[11\bar{2}0]_H \| [111]_B$, $(0002)_H \| (\bar{3}30)_B$, the ideal Burgers OR and the Dyson–Andrews OR (D–A OR), $[11\bar{2}0]_H \| [111]_B$, $(1\bar{1}00)_H \| (\bar{3}30)_B$, which was observed between ferrite and M_7C_3 carbides [36] in ferrous alloys. Obviously, the Burgers OR is much more likely to form in this alloy than the D–A OR, due to the smaller *d*-value mismatch, and the former should be the predominant OR. This is consistent with the experimental results [16]. Following the procedure used with the Mg–Al alloy, these two ORs need to be further refined using the **Δg** approach and the corresponding habit planes can also

Table 2
Atom positions in $Mg_{24}Y_5$ (ε) phase

Structure type: Mn	Pearson symbol: *cI*58	Space group: $I\bar{4}m$	Space group no. 217
Multiplicity, Wyckoff letter, Site symmetry	Coordinates: (0,0,0,)+ (0.5,0.5,0.5)+		
	x	*y*	*z*
Y1, 2*a*, $\bar{4}3m$	0	0	0
Mg1, 24g, *..m*	0.3605	0.3605	0.0259
Mg2, 24*g*, *..m*	0.0857	0.0857	0.2805
Y2, 8*c*, *.3m*	0.3126	0.3126	0.3126

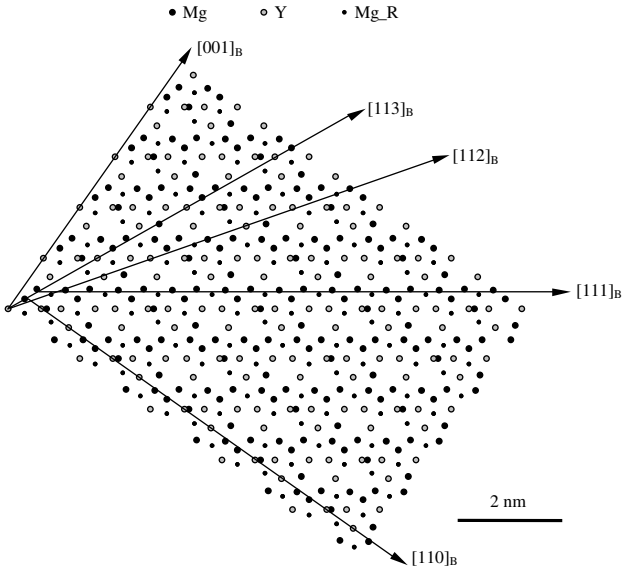

Fig. 8. Atom configuration of ε phase on $(\bar{1}10)_B$ plane at lattice parameter $a = 1.126$ nm.

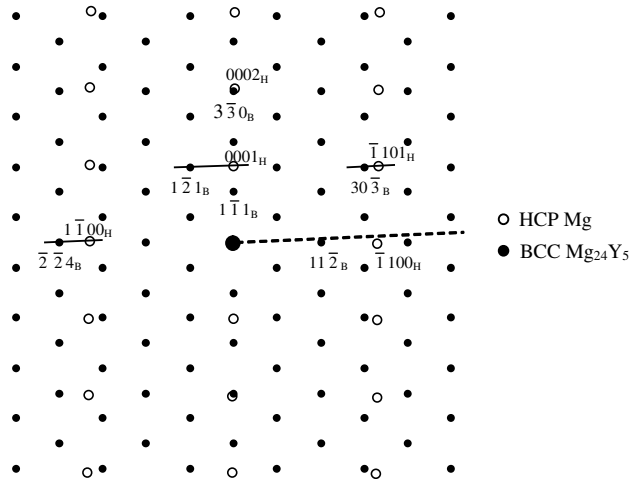

Fig. 9. Simulated diffraction patterns of Mg matrix and ε phase along the zone axis $[11\bar{2}0]_H \| [111]_B$, showing the Burgers OR and a set of parallel $\Delta\mathbf{g}$s. Dashed line indicates the habit plane.

Table 3
Interatomic spacing misfit along the possible matching directions between ε phase ($a = 1.126$ nm) and Mg matrix ($a = 0.320936$ nm, $c = 0.521123$ nm)

Directions pairs	$\langle 11\bar{2}0\rangle_H/\langle 110\rangle_B$	$\langle 11\bar{2}0\rangle_H/\langle 111\rangle_B$
Misfit (%)	20.8	3.9

be predicted. The refinement leads to the following two ORs:

$$[11\bar{2}0]_H \| [111]_B \quad (0002)_H \ 0.38^\circ \text{ from } (3\bar{3}0)_B$$
$$[2\bar{1}\bar{1}0]_H \ 5.27^\circ \text{ from } [001]_B. \tag{9}$$

The corresponding habit plane is 1.82° from $(11\bar{2})_B \| (\bar{1}100)_H$. The OR (9) is actually very close indeed to the ideal Burgers OR that has been uniquely observed between the ε phase and the Mg matrix in the Mg–Y alloy [16]. The predicted habit plane is also consistent with the experimental results [16]. Fig. 9 is the simulated diffraction pattern showing this OR and a set of parallel $\Delta\mathbf{g}$s that is normal to the habit plane.

The other OR obtained is

$$[11\bar{2}0]_H \| [111]_B \quad (1\bar{1}00)_H \ 7.8^\circ \text{ from } (\bar{3}30)_B \tag{10}$$

with a habit plane that is 7.4° from $(01\bar{1})_B$. OR (10) is an abnormal OR and has never been reported before. In fact it is less likely to form compared with the Burgers OR due to the bigger d-value mismatch between $(1\bar{1}00)_H$ and $(\bar{3}30)_B$ and the fact that $\{1\bar{1}00\}_H$ is not the closest packed plane. Hence, it is reasonable to conclude that the Burgers OR dominates crystallography of the ε phase and Mg matrix in Mg–Y alloy. Compared with the near Burgers OR between the β phase and the Mg matrix in Mg–Al alloy, the 6% increase in lattice parameter of ε phase leads to a significant change in the habit plane. Both the experimental results [16] and the predictions from the edge-to-edge matching model have demonstrated this effect very clearly.

4.4. Mg–Mn alloy

Mn has similar crystal structure to the β and ε phases and contain 58 atoms in one unit cell. The atom positions are listed in Table 5 [28]. Fig. 10 shows the atom configurations on the $(\bar{1}10)_B$ plane, which contains all possible close or near close packed directions, at the lattice parameter $a = 0.89125$ nm [25]. The notation Mn_R means the Mn atoms that are not exactly on the plane, but where the distance from the atom center to the plane is less than the atom radius. It can be seen that along the directions, $[001]_B$, $[112]_B$ and $[113]_B$, the interatomic spacing is either large or variable, therefore they will not form any ORs. The close packed direction is $[111]_B$ and the nearly close packed direction is $[110]_B$. Both can be regarded as straight atom rows. Like the

Table 4
d-value mismatch between possible matching planes corresponding to $[11\bar{2}0]_H \| [111]_B$ direction

Possible matching planes	$\{0002\}_H/\{\bar{3}30\}_B$	$\{1\bar{1}01\}_H/\{\bar{3}30\}_B$	$\{1\bar{1}00\}_H/\{\bar{3}30\}_B$
d-value mismatch (%)	1.8	7.6	4.7

For ε phase, $a = 1.126$ nm, for Mg $a = 0.320936$ nm, $c = 0521123$ nm.

Table 5
Atom position in α-Mn

Structure type: Mn	Pearson symbol: *cI*58	Space group: $I\bar{4}m$	Space group no. 217
Multiplicity, Wyckoff letter, Site symmetry	Coordinates: (0,0,0,)+ (0.5,0.5,0.5)+		
	x	*y*	*z*
Mn1, 2*a*, $\bar{4}3m$	0	0	0
Mn2, 8*c*, *.3m*	0.316	0.316	0.316
Mn3, 24*g*, *..m*	0.356	0.356	0.034
Mn4, 24*g*, *..m*	0.089	0.089	0.282

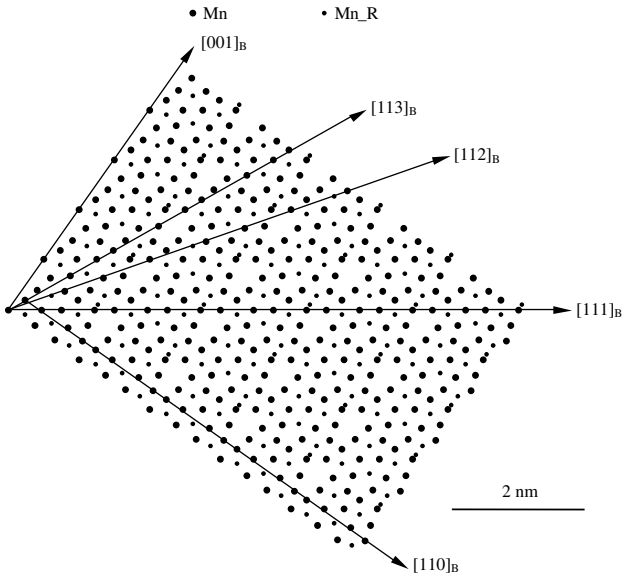

Fig. 10. Atom configuration of α-Mn on the $(\bar{1}10)_B$ plane with a lattice parameter $a = 0.89125$ nm.

system of ε phase in Mg matrix, there are only two possible matching direction pairs, $\langle 11\bar{2}0\rangle_H/\langle 110\rangle_B$ and $\langle 11\bar{2}0\rangle_H/\langle 111\rangle_B$, between the α-Mn and the Mg. Table 6 lists the interatomic misfit along these two direction pairs.

This large interatomic spacing mismatch (>20%) indicates that there are no directions pairs that can be the matching directions to form an OR between α-Mn and Mg matrix. Hence, it can be concluded that there are unlikely to be reproducible ORs between α-Mn precipitates and the Mg matrix. This implies that the interfacial boundary between α-Mn and Mg is neither coherent nor partially coherent. This is consistent with the present experimental results.

Table 6
Interatomic spacing misfit in two possible matching directions between α-Mn phase ($a = 0.89125$ nm) and Mg matrix ($a = 0.320936$ nm, $c = 0521123$ nm)

Directions pairs	$\langle 11\bar{2}0\rangle_H/\langle 110\rangle_B$	$\langle 11\bar{2}0\rangle_H/\langle 111\rangle_B$
Misfit (%)	24.2	20.1

5. Discussion

As stated above, the edge-to-edge matching model is based on the matching of actual atoms, rather than just lattice points across the interfacial boundary of two phases. Although a crystal lattice can perfectly describe the crystallographic features of the crystal, in more complex crystals there may be more than one atom associated with each lattice point. Hence, matching of lattice points at the interface does not necessarily lead to atom matching and does not result in a low interfacial energy. For simple crystal structures, such as α-Fe, γ-Fe, Cu, Al, Mg, single atoms occupy the lattice points and all the atoms in one unit cell can be allocated to the lattice points. In this case, lattice point matching and atom matching are equivalent. For most compounds, such as β and ε phases in Mg alloy, or even α-Mn metal, their crystal structure is much more complicated. Atoms not only occupy the lattice point, but also occupy other positions in the unit cells. If only lattice points are considered, up to as many as 90% of the atoms may end up being ignored. If most of the atoms are ignored during a crystallographic analysis, incorrect results and predictions may be obtained. Some previous work [1,30–33], the O-lattice model in particular, was based entirely on lattice points in an attempt to explain the interfacial structures between phases and the actual atoms in the adjacent phases were not always taken into account. Hence, this work can only explain the observed habit plane for well-established ORs between β phase and Mg matrix or between cementite and austenite in steels using the successful **Δg** theory. They are unable to predict any OR from first principles. Other work, such as the invariant line model [36–39], can only explain the observed ORs in simple crystal systems based on the one dimension matching along a direction that is supposed to be undistorted and unrotated during the phase transformation process. Most of the work using the structure ledge model [40–47] was carried out in simple systems, such as ferrite/austenite, Ti–Cr and Cu–Cr alloys. In these simple cases lattice matching is equivalent to atom matching. Hence, the model successfully explained the relationship between the atomic habit plane and the apparent habit plane for a known OR. It cannot predict OR and habit plane from first principles either.

The difference between the structure ledge model and the edge-to-edge matching model was discussed in Part I [29].

As stated above, the current edge-to-edge matching model has successfully predicted the Potter OR, the near Burgers OR and the G–O OR between the β phase and the Mg matrix, and all these ORs have been experimentally observed in Mg–Al alloys. However, for the Crawley OR and the Porter OR, it was not so successful. Previous work [1,8–12] has shown that, these ORs were observed when the precipitates lay on the prismatic planes of the Mg matrix. This implies that when the β phase obeys the Crawley OR or the Porter OR, the habit plane is different from the one corresponding to the Potter OR or the near Burgers OR that are the predominate ORs in this system. One reason for the change of habit plane is an increase in lattice parameter even though the crystal structure remains the same. Because the chemical composition of the β phase varies according to the Mg–Al phase diagram, it may result in a change of lattice parameter. Zhang and Kelly's work has confirmed the difference in lattice parameters between the near Burgers OR and the Potter OR between the β phase and the Mg matrix [13]. Our previous work [13,16] indicates that the 6% increase in lattice parameter of ε phase relative to the β phase lead to the habit plane change from the basal plane of the Mg matrix for β to the prismatic plane for the ε phase. Using the Kikuchi line diffraction patterns to determine the lattice parameter of the β phase that obeys the Crawley OR has shown that the lattice parameter has increased 4.5–6.6% compared with the β phase that obeys the near Burgers OR or the Potter OR. Hence, it is believed that the observed Crawley OR and the Porter OR between β phase and Mg matrix are associated with a lattice parameter increase. That is why these two OR could not be predicted using the current published data [25]. Due to the lack of the accurate data for the β phase that obeys the Crawley and the Porter ORs, the prediction cannot be undertaken. But these two ORs can be understood in terms of the model. Assume the lattice parameter of the β phase that obeys either the Crawley OR or the Porter OR increase 5.1%, then the *d*-value mismatch between $\{1\bar{1}00\}_H$ and $\{330\}_B$ will be less than 6% and the one between $\{0002\}_H$ and $\{330\}_B$ will over 6%. In this case the matching plane for the most preferred matching direction, $\langle 11\bar{2}3\rangle_H/\langle 113\rangle_B$, will change to $\{1\bar{1}00\}_H/\{330\}_B$ from $\{1\bar{1}01\}_H/\{330\}_B$ (see Figs. 3 and 4). The refinement using **Δg** approach gives the OR as $[11\bar{2}3]_H \| [113]_B$, $(1\bar{1}00)_H$ 2.58° from $(330)_B$, which is equivalent to the following ORs:

$$[1\bar{2}10]_H \text{ 2.2° from } [2\bar{1}\bar{1}]_B \quad (0002)_H \text{ 2.5° from } (111)_B. \tag{11}$$

The corresponding habit plane is 3.9° from $(\bar{2}111)_H$ that is at an angle of 72° to the $(0001)_H$ basal plane of the Mg matrix. This OR is very close to the reported Crawley OR and there is good agreement between the predicted habit planes and the experimental results. The Porter OR may be generated from different matching directions associated with the matching plane, $\{1\bar{1}00\}_H/\{330\}_B$. As shown in Fig. 2 there is one zigzag atom row that deviates 14.5° from the $[100]_B$ direction. When the lattice parameter of the β phase is changed, this atom row and the zigzag atom row along $[11\bar{2}3]_H$ direction may form a matching direction pair. The combination of this matching direction, $[11\bar{2}3]_H$ 14.51° from $[100]_B$ and the matching plane, $(1\bar{1}00)_H \| (033)_B$, gives rise to the exact Porter OR.

Although this analysis may well explain the Crawley OR and the Porter OR, it is not really a predicted result. To predict the ORs between the Mg and the β phase for precipitates at an angle to the basal plane of Mg, the accurate lattice parameter of the β phase must be known.

OR (3) and OR (4) are two different the near Burgers ORs. Both involve deviation of about 0.5° between $[2\bar{1}\bar{1}0]_H$ and $[111]_B$. But the deviation direction is different in the two cases. If γ denotes the angle between $[11\bar{2}0]_H$ and $[001]_B$ in the OR, the ideal Burgers OR corresponds to $\gamma = 5.26°$, OR (3) corresponds to $\gamma = 4.76°$ and OR (4) to $\gamma = 5.76°$. Duly et al. [1] have reported the OR (4) between β phase and the Mg and considered it to be the true OR in the system, while the reported ideal Burgers OR is the consequence of experimental errors. Further analysis of the experimental results published in [13] after transforming all the determined ORs into the same variant, shows that the angle γ can be either over 5.26° or below this value. Fig. 11 shows the experimental results showing the measured γ angle. Hence, it appears that both the OR (3) and OR (4) exist as ORs between β and the Mg matrix. These two ORs have been regarded as the ideal Burgers OR in most previous research due to the limited accuracy of the selected area diffraction technique used to determine the OR. In fact all the observed Burgers ORs are probably one of these two ORs.

Another important issue that should be discussed is the fact that the predicted habit planes for OR (3) and OR (4) do not agree with the experimentally determined results. The latter shows clearly that the habit plane corresponds to the basal plane of the Mg matrix. The prediction for the OR (3) is close to this plane, but the predicted habit plane for OR (4) is not. In the edge-to-edge matching model, the plane calculated using the **Δg** approach is actually the intersection plane between two phases where the matching planes meet edge-to-edge. This plane normally represents a fully or partially coherent plane. According to the model [17,27], for a given precipitate, there are two possible interfaces with the matrix that can be the broad face or habit plane. One is the intersection plane of the matching plane and another

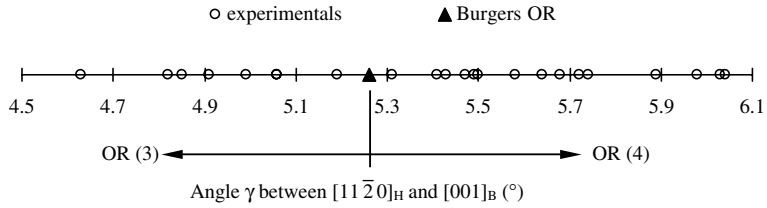

Fig. 11. Experimental results showing the angle γ between $[11\bar{2}0]_H$ and $[001]_B$ for the OR (4) and OR (3) compared with the ideal Burgers OR.

is the matching plane itself. Which plane will grow into the broad face depends on the competition between the surface energy on the matching plane, which is in contact with the matrix, and the strain energy across the partially coherent interface, which is the intersection plane of the matching planes. The driving force for an interface to be fully or partially coherent is to lower the surface energy from that of a totally incoherent interface. But when there is misfit and mismatch across this interface, strain energy will be generated. If the strain energy increase is smaller than the reduction in surface energy, this fully or partially coherent interface, which is the intersection plane of the matching planes, will grow into the broad face. In this case, the observed habit plane will be consistent with the predictions. If the misfit and mismatch across the partially coherent interface is larger and leads to an increase in strain energy that exceeds the reduction in surface energy, the matching plane itself may grow into the broad face. This is particularly likely if the matching plane itself has a low surface energy. In this case, the observed habit plane will be the matching plane itself. In OR (3) and OR (4), the matching directions are the pure zigzag row in the Mg matrix and a partially zigzag, partially straight row in β phase, as shown in Fig. 2, and this will definitely result in larger misfit along the matching directions. Therefore, as the growth of the β precipitates, the strain energy on this partially coherent plane increases. When this strain energy exceeds the surface energy, the partially coherent interface will stop growing, allowing another interface to develop as the broad face of the precipitate. Because the $\{0002\}_H$ and $\{330\}_B$ planes are the closest packed planes in both phases, they correspond to the lowest surface energy and are favored to become the broad face. Hence, in previous work, the observed Burgers OR was associated with the $(0001)_H$// $\{330\}_B$ habit plane. It should also be emphasized that the previously determined Burgers OR was actually the near Burgers OR.

The predicted ORs (5), (7) and (8) have never been experimentally observed. This is due to the large interatomic spacing misfits along their matching directions as shown in Fig. 3. These ORs are much less likely to occur, particularly when there are other matching directions, along which the interatomic spacing misfit is much smaller. Hence, these ORs should be very rare or never observed in this system, unless the lattice parameter or the atom positions change in a way that reduces the misfit along the matching directions.

6. Conclusions

(1) According to the predictions of the edge-to-edge matching model, the Potter OR and the near Burgers OR are two major ORs between the β phase and the Mg matrix in an Mg–Al alloy. Other ORs, such as the Porter OR, the Crawley OR and the Gjönnes–Östmoe OR, are occasionally observed in this system. This agrees very well with the results from previous and present work. In addition, the predicted habit planes for these ORs are consistent with the experimental results.

(2) In the Mg–Y system, the model predicts that the only OR between the phase and the Mg matrix is the Burgers OR with habit plane $\{10\bar{1}0\}_H \| \{112\}_B$. This is completely consistent with the experimental results.

(3) Both the model and the experimental work demonstrate that there is no reproducible OR between α-Mn and Mg matrix in Mg–Mn alloy.

(4) The model is based on the actual atom row matching across the interface. Therefore to use the model, the crystal structure, the lattice parameters and the atom positions in one unit cell are the only input data required. To predict the ORs, the interatomic spacing misfit along the matching directions has to be calculated and must be smaller than 10%. In addition, the *d*-value mismatch between the matching planes that contain the matching directions must be less than 6%. The habit plane can be either the matching planes themselves or the intersection plane of the matching planes. The latter can be determined using the $\Delta\mathbf{g}$ theory.

Acknowledgements

The authors are grateful to the Australian Research Council (ARC) Large Grant for funding support and

to Prof. Wenzheng Zhang for her considerable help in explaining the details of the **Δg** theory.

References

[1] Duly D, Zhang W-Z, Audier M. Philos Mag 1995;71:187.
[2] Nie JF, Muddle BC. Acta Mater 2000;48:1691.
[3] Aghion E, Bronfin B. Mater Sci Forum 2000;350–351:19.
[4] Kim W-J, Chung SW, Chung CS, Kum D. Acta Mater 2001;49:3337.
[5] Ma Q, Zheng L, Graham D, Frost MT, StJohn DH. J Light Metals 2001;1:157.
[6] Froes HF, Eliezer D, Aghion E. JOM 1998;9:30.
[7] Luo AA. Materials comparison and potential applications of magnesium in automobiles. In: Kaplan HI, Hryn JN, Clow BB, editors. Magnesium technology. Warrendale (PA): TMS; 2000. p. 89.
[8] Clark JB. Acta Metall 1968;16:141.
[9] Crawley AF, Milliken KS. Acta Metall 1974;22:557.
[10] Crawley AF, Lagowski B. Metall Trans A 1974;5:949.
[11] Duly D, Brechet Y. Acta Metall Mater 1994;42:3035.
[12] Celotto S. Acta Mater 2000;48:1775.
[13] Zhang M-X, Kelly PM. Scripta Mater 2003;48:647.
[14] Zhang M-X, Kelly PM. Charact Mater 1999;43:11.
[15] Zhang M-X, Kelly PM. Charact Mater 1998;40:159.
[16] Zhang M-X, Kelly PM. Scripta Mater 2003;48:379.
[17] Kelly PM, Zhang M-X. Mater Forum 1999;23:41.
[18] Duly D. Acta Metall Mater 1993;41:1559.
[19] Porter DA, Edington JW. Proc R Soc A 1977;358:335.
[20] Zhang M-X, Kelly PM. Acta Mater 1998;46:4081.
[21] Zhang M-X, Kelly PM. Acta Mater 1998;46:4617.
[22] Duly D, Cheynet MC, Brechet Y. Acta Metall Mater 1994;42:3843.
[23] Vegard L. Z Physik 1921;5:17.
[24] Hardie D, Parking RN. Philos Mag 1959;4:815.
[25] JCPDS – International Centre for Diffraction Data, PCPDFWIN v. 2.3.
[26] ASM handbook, Alloy phase diagram, vol. 3. Materials Park (OH): ASM International; 1992.
[27] Kelly PM, Zhang M-X. Metall Mater Trans 2005, in press.
[28] Villars P, Calvert LD. Pearson's handbook of crystallographic data for intermetallic phases, vol. 1. Materials Park (OH): ASM International; 1991. pp. 905, 4317, 4321.
[29] Zhang M-X, Kelly PM. Edge-to-edge matching and its applications. Part I. Application to the simple HCP/BCC system. Acta Mater 2005, this issue.
[30] Zhang W-Z, Purdy GR. Acta Metall Mater 1993;41:543.
[31] Zhang W-Z, Purdy GR. Philos Mag 1993;68:279.
[32] Zhang W-Z, Ye F, Zhang C, Qi Y, Fang H-S. Acta Mater 2000;48:2209.
[33] Ye F, Zhang W-Z. Acta Mater 2002;50:2761.
[34] Zhang W-Z. Use of D-lattice for study of crystallography of phase transformations. In: Koiwa M, Otsuka K, Miyazaki T, editors. Proc Int Conf Solid-solid Phase Transformations. Part 1. Sendai: Japan Institute of Metals; 1999. p. 581.
[35] Ye F, Zhang W-Z, Qiu D. Acta Mater 2004;52:2449.
[36] Dahmen U. Acta Metall 1982;30:63.
[37] Dahmen U. Scripta Metall 1981;15:77.
[38] Dahmen U. Metall Mater Trans 1994;25A:1857.
[39] Luo CP, Dahmen U, Westmacott KH. Acta Metall Mater 1994;42:1923.
[40] Hall MG, Aaronson HI, Kinsman KR. Surf Sci 1972;31:257.
[41] Rigsbee JM, Aaronson HI. Acta Metall 1979;27:351–65.
[42] Furuhara T, Howe JM, Aaronson HI. Acta Metall Mater 1991;39:2873.
[43] Furuhara T, Aaronson HI. Acta Metall Mater 1991;39:2887.
[44] Russell KC, Hall MG, Kinsman KR, Aaronson HI. Metall Trans A 1974;5:1503.
[45] Hirth JP. Metall Mater Trans A 1994;25:1885.
[46] van der Merwe JH, Shiflet GJ. Acta Metall Mater 1994;42:1173. 1189 and 1199.
[47] Shiflet GJ, van der Merwe JH. Metall Mater Trans A 1994;25:1895.